Proceedings of The Magnetized Plasma in Galaxy Evolution
Sep. 27th – Oct. 1st 2004, Jagiellonian University, Kraków, Poland
Eds. K.T. Chyży, K. Otmianowska-Mazur, M. Soida and R.-J. Dettmar

Anisotropic Wavelet Analysis of Spiral Arms and Magnetic Fields in the Galaxy M51

Igor Patrickeyev[1], A. Fletcher [2,3], R. Beck.[2], E. M. Berkhuijsen[2], P. Frick[1], and C. Horellou[4]

[1]Institute of Continuous Media Mechanics, Korolyov str. 1, Perm, Russia
[2]Max-Planck-Institut für Radioastronomie, Auf dem Hügel 69, 53121 Bonn, Germany
[3]School of MathemaTICS & Statistics, University of Newcastle, Newcastle, NE1 7RU, U.K.
[4]Onsala Space Observatory, Chalmers University of Technology, Onsala, Sweden

Abstract

The choice of mathematical tool is of great importance in image analysis. For images with extended structures, such as galactic spiral arms, the anisotropic wavelet transform, based on space-scale-direction decomposition, is a powerful tool. It can be considered a generalization of the isotropic wavelet transform by introducing a rotation operator in addition to the translation and dilation operators. Such an elaboration gives new possibilities to track elongated spiral-shaped structures. Application to a CO map of the galaxy M51 quantify the local pitch angle of arms of molecular gas, without assuming a particular global form of the structure, e.g. a logarithmic spiral. We have compared the obtained pitch angles with the orientation of the regular magnetic field. Preliminary results are: 1) the pitch angles of the gaseous spiral arm and of the regular magnetic field on the arms are generally aligned, 2) there are signs of systematic shifts in some regions, where the field has a smaller pitch angle than the CO arm.

1 Introduction

A new method, proposed in this work, quantifies the pitch angle of spiral arms. It is based on self-similar functions, which are well-localized both in the physical and Fourier domain and non-invariant to rotation. These functions are called anisotropic wavelets.

The first applications of wavelets to galactic image analysis showed many advantages of this tool for detection and evaluation of galaxy parameters. In recent applications one-dimensional (Frick et al. 2000) and two-dimensional isotropic wavelets (Frick et al. 2001) have been used.

With the advent of new fast computers a better suited tool to analyze an image with directional structure is available. In this study, we have applied a two-dimensional *anisotropic* wavelet transform to the galaxy M51. We have used this transform to evaluate the pitch angles of the arms of molecular gas, studied the radial variation of the pitch angles and compared it with the orientation of the regular magnetic field.

2 The data

M51 is a grand-design spiral galaxy with two major arms threaded with an intricate pattern of dust lanes. The galaxy is probably interacting with a companion galaxy. Interactions usually involve an enhancement of localized star formation rates as shear forces compress the gas and dust (Howard et al. 1990). The two principle arms can be traced through more than 360° in azimuth. In the arms, as well as in discrete H II regions, there are large blobs or bubbles, rich in H II.

Data in many spectral ranges are available. For our analysis we used the (1-0) line emission of the carbon monoxide molecule (CO) at the wavelength 2.6 mm observed with the BIMA interferometer and corrected for missing spacings with single dish observations, integrated over the whole frequency width of the line (Helfer et al. 2003). The CO emission is the best available tracer of the *molecular gas* in galaxies. The polarized radio continuum emission from M51 at 3 cm and 6 cm wavelengths has been observed with the VLA and Effelsberg telescopes (Fletcher et al. 2004). Here we use the 6 cm data which have higher signal-to-noise values.

3 The method: anisotropic wavelets

A wavelet transform is the convolution of an image with a family of wavelets having three parameters: location, size and orientation. The family of basic functions is generated by translations, dilations and rotations of the mother function. One-dimensional and isotropic multi-dimensional wavelet transforms are based on the space-scale decomposition of the signal. Using a continuous wavelet transform, the result of image decomposition is a 3D cube. Cross-sections of the cube are slices which emphasize details of a fixed scale. Each slice has the same number of pixels as the original image. As a result, the wavelet transform conserves local properties of the image.

In addition to translation and dilation, the anisotropic wavelet transform involves rotation of the mother wavelet to generate a family of basic functions. An anisotropic wavelet transform converts an image to a 4D set, which is a space-scale-orientation decomposition. Fixed space and scale parameters give the possibility to track orientational properties of elongated structures. In our work, this property is exploited to analyze the orientation of the spiral arms.

3.1 The Texan Hat function

We introduce a new two-dimensional (2D) anisotropic wavelet, called the Texan Hat function (TH), which in the simplest form is the second partial derivative of the 2D isotropic Gaussian function in y, taken with the negative sign:

$$TH(x,y) = \left(1 - y^2\right) \exp\left(-\frac{x^2+y^2}{2}\right). \tag{1}$$

The function TH meets the conditions wherein this function can be called a wavelet: it has a mean value of zero, it is well localized both in the physical and Fourier spaces and it meets the admissibility condition (Holschneider 1995). The results presented in this work have been obtained using the simplest form of the TH, defined by equation (1).

3.2 Performing transforms

Applying the dilation operator $D_a[f(x,y)] = f(x/a, y/a)$ we can expand (at $a > 1$) or compress ($0 < a < 1$) the wavelet. The rotation operator $R_\phi[f(x,y)] = f(x\cos\phi + y\sin\phi, -x\sin\phi +$

$y\cos\phi$) changes the orientation of the wavelet. As a result of dilation and rotation we obtain a family of wavelets of different sizes and orientations:

$$TH_{a,\phi}(x,y) = \left(1 - \frac{(y\cos\phi - x\sin\phi)^2}{a^2}\right)\exp\left(-\frac{x^2+y^2}{2a^2}\right). \qquad (2)$$

We use the 2D *continuous* wavelet transform (Antoine et al. 1999), which is expressed in the form

$$w(a,x,y,\phi) = \frac{1}{a^2}\int_{-\infty}^{+\infty}\int_{-\infty}^{+\infty} f(x',y')TH_{a,\phi}\left(x-x',y-y'\right)dx'dy'. \qquad (3)$$

Here $f(x,y)$ is a two-dimensional function and w is the result of wavelet transformation hereafter called "wavelet transform at point (x,y)" or just "wavelet coefficients".

The wavelet transform (3) is unique and reversible which means that the analyzed function $f(x,y)$ can be reconstructed from its wavelet coefficients. Sometimes, the process of obtaining wavelet coefficients is called "wavelet analysis" and the process of reconstruction from the wavelet coefficients "wavelet synthesis". In our work, we use only wavelet analysis and do not use a reconstruction formula. (An extended description of the continuous wavelet transform can be found in Holschneider 1995 and Torresani 1995.)

3.3 Tracking of elongated structures with the Texan Hat

Directional properties of the anisotropic wavelet can be used to quantify the structure orientation. The accuracy of the quantification depends on how well the structure is elongated. For a non-elongated structure (e.g. circle) we can not define orientation. A typical spiral arm is an example of "elongated structure": its transverse size is much less than its length.

Analysis of the map is made point-by-point. At some points we obtain negative wavelet coefficients which can be explained by shifting the proper oriented wavelet across the structure. When the wavelet is localized at the edge of the arm, the area under the positive part is almost the same as under the negative one, and the wavelet coefficient is roughly equal to zero. Negative wavelet coefficients can be considered as a result of location of the TH center outside the structure.

4 Results

Figure 1 presents the original CO map of M51 (Helfer et al. 2003) and the map of maximal wavelet coefficients for all scales. The strong two-armed spiral pattern visible in the original CO map means that at all radii there are two distinct maxima in the wavelet coefficients corresponding to the positions of the spiral arm (Fig. 1), i.e. there are no bright, elongated, inter-arm clouds that produce a high wavelet coefficient. The pitch angles of the arms traced by CO emission were measured by the anisotropic wavelet method described in Section 3, taking the pitch angle at the *two* maxima in wavelet coefficients at a given radius.

Observations of nearby spiral galaxies suggest that the regular magnetic field generally has a pitch angle similar to that of the spiral arms (Beck et al. 1989, Rohde et al. 1999, Frick et al. 2000). Using the proposed method we can quantify how close the alignment is. Figure 2 shows the pitch angles along the two spiral arms of M51, for the molecular gas traced by CO emission (Helfer et al. 2003) and for the regular magnetic field obtained from radio polarization observations (Fletcher et al. 2004). Both data sets are a combination of

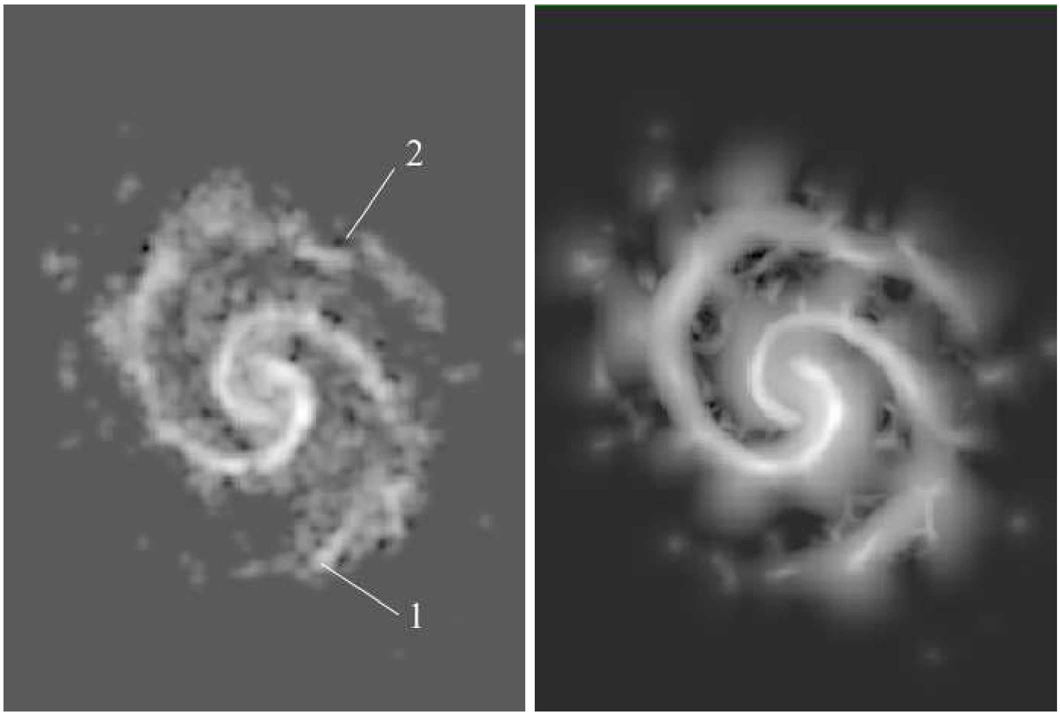

Figure 1: *(left)* Original map of CO (1-0) in M51 (Helfer et al. 2003) and *(right)* maximal wavelet coefficients of CO. Intensity is in logarithmic scale. Arms 1 and 2 are indicated.

interferometer and single dish observations and so should not suffer from missing large-scale flux. The orientation of the linearly polarized emission used to measure the magnetic field pitch angles was corrected for the Faraday rotation and both datasets were smoothed to $8''$ resolution.

The pitch angles of the regular magnetic field were determined from the observed Stokes Q & U at the points of the maxima in the wavelet coefficients of the transformed CO map; the magnetic field pitch angles in Fig. 2 are therefore the *pitch angles of the regular magnetic field on the spiral arms.* The errors in magnetic field pitch angle are determined using the noise in the observed maps only and do not include any systematic effects such as uncertainty in the galaxy inclination. Note that between $3.0 < r < 3.9$ kpc in the upper panel of Fig. 2 no magnetic field pitch angles are shown. This is because no polarization is detected in this region; at smaller and higher radii the regular field is strong at the position of the CO arm, but in this 0.9 kpc section the regular magnetic field cannot be traced by the wavelet transform method.

Figure 2 shows a marked scatter in the pitch angles of both gaseous spiral arms and magnetic field. Although the pitch angles of the CO arms and the magnetic field are roughly of the same magnitude, in 21 out of 36 positions the measured angles do not agree within errors; the discrepancy between CO arm and magnetic field pitch angles in these cases is typically $\sim 10°$.

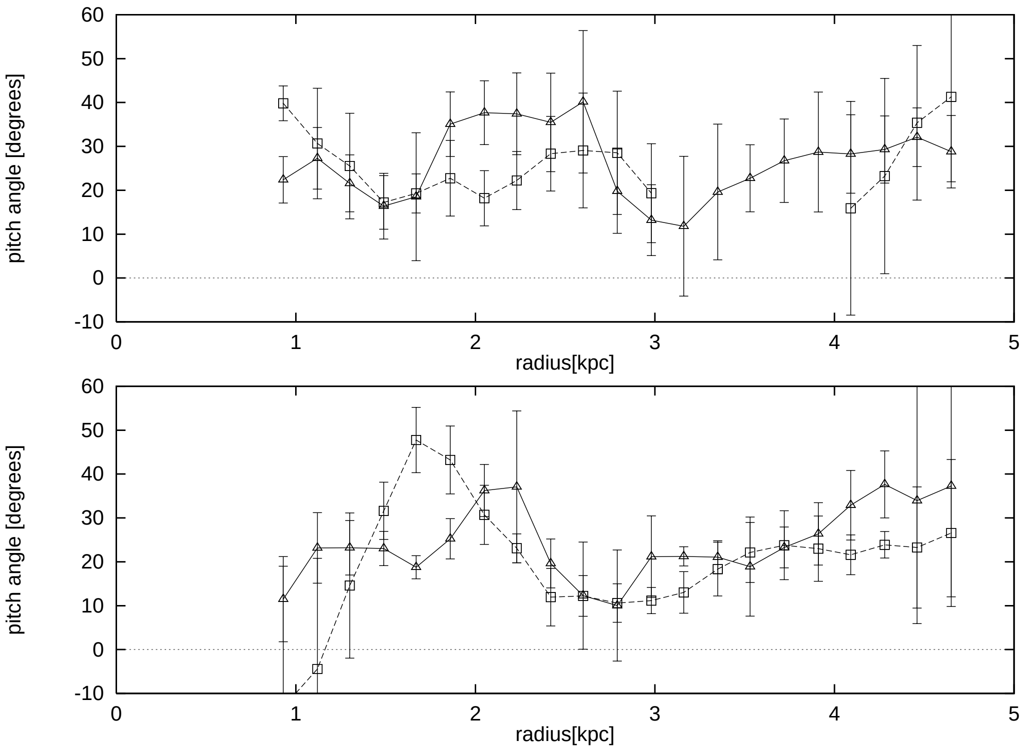

Figure 2: Radial variation of the CO and regular magnetic field pitch angles for spiral arm 1 (see Fig. 1) (*upper panel*) and arm 2 (*lower panel*). The CO pitch angles (*triangles*) were obtained using the anisotropic wavelet method by selecting two highest wavelet coefficients at a given radius. The regular magnetic field pitch angles (*boxes*) show the orientation of the large scale field at the same position as the selected pitch angle of CO in the two spiral arms.

5 Conclusions

The CO arms and both regular magnetic field spirals of the galaxy M51 are not logarithmic spirals, *i.e. the pitch angle is not constant.* This is the case even if we ignore the outer magnetic spiral in arm 2, which obviously has a higher pitch angle than the inner magnetic field, and consider only the radial range $0.9 < r < 2.8$ kpc. The error-weighted average pitch angles are $\sim 26°$ for the CO of arm 1 and $\sim 20°$ for the magnetic field along arm 1, $\sim 24°$ for the CO of arm 2 and $\sim 21°$ for the magnetic field along arm 2. The pitch angles in Fig. 2 show a tendency in some regions of the magnetic field to have a lower (more tightly wound or azimuthal) pitch angle than that of the gaseous arms.

Acknowledgements

We thank A. Shukurov and R. Stepanov for useful discussion and for helpful comments. This work was supported through cooperative grant DFG (436RUS113/772) – RFBR (03-02-04031). Igor Patrickeyev is grateful to the organizing committee of the conference for support and hospitality.

References

Antoine, J. P., Carette, P., Murenzi, R., & Piette, B., 1993, Signal Processing, 31, 241

Beck, R., Loiseau, N., Hummel, E., Berkhuijsen, E. M., Gräve, R., & Wielebinski, R., 1989, A&A, 222, 58

Fletcher, A., Beck, R., Berkhuijsen, E. M., Horellou, C., & Shukurov, A., 2004, in: *How Does the Galaxy Work?*, ed. E. J. Alfaro et al. (Dordrecht: Kluwer), p. 299

Frick, P., Beck, R., Shukurov, A., Sokoloff, D., Ehle, M., & Kamphuis, J., 2000, MNRAS, 318, 925

Frick, P., Beck, R., Berkhuijsen, E. M., & Patrickeyev, I., 2001, MNRAS, 327, 1145

Helfer, T. T., Thornley, M. D., Regan, M. W., Wong, T., Sheth, K., Vogel, S. N., Blitz, L., & Bock, D. C. J., 2003, ApJS, 145, 259

Holschneider, M., 1995, *Wavelets: An Analysis Tool* (Oxford: Oxford University Press)

Howard, S., & Byrd G., 1990, AJ, 99, 1798

Rohde, R., Beck, R., & Elstner, D., 1999, A&A, 350, 423

Torresani, B., 1995, *Continuous Wavelet Transform* (Paris: Savoire)